ORIGINAL SCIENTIFIC PAPER

Croat. Chem. Acta 2017, 90(4), 711–725
Published online: April 24, 2018
DOI: 10.5562/cca3308

Synthesis of Fluorescent Diphenylanthracene-Based Calix[4]arene Derivatives and their Complexation with Alkali Metal Cations

Marina Tranfić Bakić,[1,#] Katarina Leko,[2,#] Nikola Cindro,[2] Tomislav Portada,[3] Tomica Hrenar,[2] Leo Frkanec,[3] Gordan Horvat,[2] Josip Požar,[2] Vladislav Tomišić[2,*]

[1] Laboratory of Physical Chemistry and Corrosion, Faculty of Food Technology and Biotechnology, University of Zagreb, Pierottijeva 6, HR-10000 Zagreb, Croatia
[2] Division of Physical Chemistry, Faculty of Science, University of Zagreb, Horvatovac 102a, HR-10000 Zagreb, Croatia
[3] Laboratory of Supramolecular Chemistry, Ruđer Bošković Institute, Bijenička cesta 54, HR-10000 Zagreb, Croatia
* Corresponding author's e-mail address: vtomisic@chem.pmf.hr

RECEIVED: February 14, 2018 ⋆ REVISED: April 23, 2018 ⋆ ACCEPTED: April 23, 2018

THIS PAPER IS DEDICATED TO PROF. MLADEN ŽINIĆ ON THE OCCASION OF HIS 70TH BIRTHDAY

Abstract: Two novel fluorescent calix[4]arenes comprising diphenylanthracene moiety at the lower rim were synthetized and their complexation with alkali metal cations in acetonitrile/dichloromethane and methanol/dichloromethane mixtures (φ = 0.5) was studied experimentally and by classical molecular dynamics and quantum chemical calculations. The monosubstituted calixarene derivative (**L1**) proved to be a poor cation receptor, whereas the ester-based macrocycle (**L2**) exhibited rather high affinity towards lithium, sodium and potassium cations, particularly in MeCN/CH_2Cl_2. All complexation reactions were enthalpically controlled, whereby the overall stability was the largest in the case of sodium complex. The computational investigations provided an additional insight into the complexation properties and structures of complex species. The molecular dynamics simulations indicated the occurrence of inclusion of solvent molecules in the calixarene hydrophobic cavity of the free and complexed ligand, which was found to significantly affect the complexation equilibria.

Keywords: calixarenes, diphenylanthracene, alkali metal cations, fluorescence, complexation, thermodynamics.

INTRODUCTION

THE hosting abilities of calixarene-based compounds have been extensively studied during the past several decades.[1] This is due to the straightforward functionalization of their upper and/or lower rims which enables the preparation of effective receptors for wide array of cations, anions and neutral species.[2–5] Calixarenes derivatives can hence be used as ion extraction reagents,[6–8] electrochemical and fluorescence sensors,[9–11] biomimetics, drug-delivery systems,[12] ion channels[13,14] and nanomaterial components.[15,16]

The lower-rim calixarene derivatives possessing electron-rich functional groups (esters, ketones or amides) have been widely used as alkali and alkaline earth metal cations complexation agents.[2–4] Owing to well-defined binding site and the possibility of fine tuning of calixarene-cation size compatibility, a remarkable stability and even selectivity towards particular cation can be achieved. Apart from that, the complexation process is strongly influenced by the solvation of both reactants and complexes formed.[4,17–25] In this context, the inclusion of solvent molecules in the macrocycle hydrophobic cavity can play an important role in the cation hosting.[20–22,24,26,27] The extent of complexation reactions in non-aqueous solvents can also be significantly affected by the process of ion pairing.[4,11]

Among the vast variety of calixarene derivatives, those bearing suitable binding sites as well fluorescent functionalities (*e.g.* anthracene, naphthalene, pyrene, dansyl, phenanthridine or tryptophan groups) have been recognized as potentially very sensitive ionic sensors, which can be attributed to the high sensitivity of fluorimetry.[9,11,28–30]

# These authors contributed equally to this work.

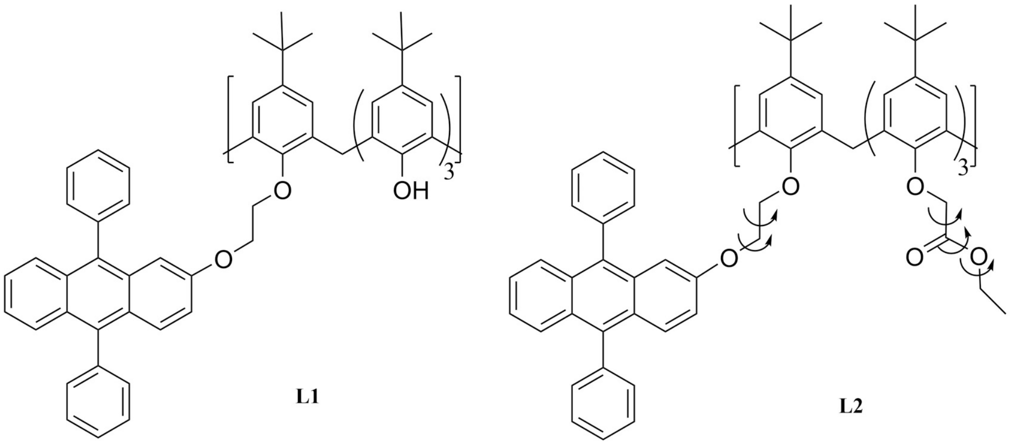

Figure 1. Structures of compounds **L1** and **L2**.

In the present work we report the synthesis of two novel calix[4]arene derivatives with diphenylanthracene subunits at the lower rim (**L1** and **L2**, Figure 1). The binding affinities of these compounds towards alkali metal cations in acetonitrile/dichloromethane ($MeCN/CH_2Cl_2$) and methanol/dichloromethane ($MeOH/CH_2Cl_2$) solvent mixtures were comprehensively studied by means of several experimental (UV and fluorescence spectroscopies, potentiometry and microcalorimetry) and computational (classical molecular dynamics and quantum chemical calculations) techniques. Such an approach provided a rather detailed thermodynamic and structural information regarding the studied complexation reactions.

EXPERIMENTAL

Synthesis

GENERAL

All reagents used in the synthesis (5,11,17,23-tetra-*tert*-butyl-25,26,27,28-tetrahydroxycalix[4]arene, potassium carbonate, potassium iodide, 1,2-dibromoethane) were purchased from Aldrich and were used without further purification. Solvents were purified by standard procedures.[31] Microwave-assisted syntheses were carried out in the Milestone START S Microwave Labstation. Reaction course and purity of the products were checked by thin-layer chromatography (TLC) on Merck, DC-Alufolien Kieselgel 60 F254. Melting points were determined with a Kofler apparatus. ^{1}H NMR and ^{13}C NMR spectra were recorded on a Bruker Avance AV300 or AV600 MHz spectrometer with TMS as an internal standard. IR spectra were recorded by means of an ABB Bomem MB102 FTIR spectrometer. High-resolution mass spectrometry (HRMS) measurements were conducted on a 4800 MALDI TOF/TOF Analyzer, Applied Biosystems mass spectrometer. 2-hydroxyanthraquinone and 9,10-diphenylanthracene-2-ol were prepared by modification of a known procedures described in Supporting Information.

2-(2-bromoethoxy)-9,10-diphenylanthracene: 9,10-diphenylanthracene-2-ol (1 g, 2.88 mmol) was dissolved in 100 mL of dry acetonitrile. To this solution potassium carbonate (1.2 g, 8.67 mmol) and dibromoethane (40 mL, 87.20 g, 467 mmol) were added. After stirring at reflux for 24 h, the reaction mixture was evaporated and partitioned between dichloromethane and water. Layers were separated, and water layer was extracted twice with dichloromethane (V = 100 mL). Organic layers were combined, dried over sodium sulfate, filtered and evaporated. The obtained residue was purified by column chromatography on SiO_2 and eluted with 1 % MeOH in DCM, yielding 810 mg (62 %) of pure product.

^{1}H NMR ($CDCl_3$, 300 MHz); δ_H / ppm: 3.59 (t, 2H, –CH_2Br); 4.17 (t, 2H, O–CH_2); 6.86 (d, 1H, J = 2.4 Hz); 7.04 (d, 1H, J = 9.4 Hz, J = 2.7 Hz); 7.30 (m, 2H); 7.46-7.48 (m, 4H); 7.52-7.67 (m, 9H). ^{13}C NMR ($CDCl_3$, 150 MHz); δ_C / ppm: 29.0; 67.5; 104.1; 119.6; 124.3; 125.2; 126.5; 126.6; 127.1; 127.5; 127.5; 128.4; 128.6; 128.8; 129.1; 130.5; 130.7; 131.2; 131.23; 135.12; 137.3; 139.0; 139.2; 155.1. FTIR (KBr) $\tilde{\nu}_{max}$ / cm^{-1}: 3058, 3029, 2962, 2925, 2854, 1625, 1610, 1492, 1479, 1452, 1380, 1280, 1222, 1211, 605 HRMS m/z $[M]^+$: 452.0786, calculated for $C_{28}H_{21}BrO$: 452.0776.

5,11,17,23-tetra-*tert*-butyl-25-(9,10-diphenylanthracene-2-yloxyethoxy)-26,27,28-trihydroxycalix[4]arene (L1): Potassium carbonate (0.68 g, 4.9 mmol), potassium iodide (0.27 g, 1.6 mmol), and 5,11,17,23-tetra-*tert*-butyl-25,26,27,28-tetrahydroxycalix[4]arene (0.36 g, 0.6 mmol) were suspended in 18 cm^3 of dry acetonitrile and stirred under reflux in argon atmosphere for about 2 h. Afterwards, 2-(2-bromoethoxy)-9,10-diphenylanthracene (0.31 g, 0.7 mmol) was added to the reaction mixture and stirred under reflux for 24 h, protected from sunlight, followed by further stirring at room temperature for another 4 days. Reaction mixture was evaporated, and water was added to the residue. The yellow precipitate was filtrated and recrystallized from ethanol yielding 220 mg (36 %) of pure compound.

Compound **L1** was also prepared by microwave-assisted synthesis. In 10 cm^3 of acetonitrile, 2-(2-bromethoxy)-9,10-diphenylanthracene (0.14 g, 0.3 mmol), potassium carbonate (0.65 g, 4.7 mmol), 5,11,17,23-tetra-*tert*-butyl-25,26,27,28-tetrahydroxycalix[4]arene (0.10 g, 0.2 mmol) and potassium iodide (0.21 g, 1.3 mmol) were suspended. Reaction mixture was stirred for 2 h at 82 °C in microwave reactor. Crude reaction mixture was filtered and washed with dichloromethane. The filtrate was evaporated and the dry residue was portioned between dichloromethane and water. Organic layer was separated and evaporated under reduced pressure leaving crude product which was purified by preparative chromatography in hexane/dichloromethane (1:1) as eluent, yielding 90 mg (56 %) of pure product.

m. p. 155–157 °C. IR (KBr) $\tilde{\nu}_{max}$ / cm^{-1}: 3329, 3055, 2957, 2870, 1627, 1455, 1484, 1391, 1364, 1293, 1205, 1125, 999, 942, 872, 753, 703. ^1H NMR ($CDCl_3$, 600 MHz); δ_H / ppm: 1.19 (s, 9H, C–$(CH_3)_3$); 1.20 (s, 18H, C–$(CH_3)_3$); 1,20(s,9H, C–$(CH_3)_3$); 3.36 (d, 2H, J = 5.6 Hz, Ar–CH_2–Ar, H_a); 3.39 (d, 2H, J = 4.9 Hz, Ar–CH_2–Ar, H_a); 4.18 (d, 2H, J = 13.6 Hz, Ar–CH_2–Ar, H_b); 4.42 (m, 2H, O–CH_2–CH_2–O); 4.45 (d, 2H, J = 13.0 Hz, Ar–CH_2–Ar, H_b); 4.48 (m, 2H, O–CH_2–CH_2–O); 6.96 (d, 2H, J = 2.2 Hz); 7.00 (s, 2H); 7.02 (d, 1H, J = 2.4 Hz); 7.03 (d, 2H, J = 2.3 Hz); 7.08 (s, 2H); 7.19 (dd, 1H, J = 9.5 Hz, 2.5 Hz); 7.26-7.33 (m, 2H); 7.47-7.49 (m, 2H); 7.52-7.54 (m, 4H); 7.55-7.67 (m, 7H); 9.32 (s, 2H, –OH); 10.10 (s, 1H, –OH). ^{13}C NMR ($CDCl_3$, 150 MHz); δ_C / ppm: 17.9; 30.5; 30.7; 30.9; 31.0; 31.2; 31.6; 32.45; 58.0; 65.6; 73.6; 103.3; 119.5; 123.7; 124.7; 125.1; 125.2; 125.4; 126.0; 126.0; 126.2; 126.6; 127.0; 127.0; 127.2; 127.9; 128.2; 128.3; 128.6; 130.0; 130.3; 130.8; 133.1; 134.7; 136.8; 138.6; 138.8; 142.5; 142.9; 143.9; 147.4; 147.8; 147.8; 148.78; 155.0. HRMS m / z [**L1**+H]$^+$: 1020.5682, calculated for $C_{77}H_{76}O_5$: 1020.5687.

5,11,17,23-tetra-*tert*-butyl-25-(9,10-diphenylanthracene-2-yloxyethoxy)-26,27,28-tris(ethyloxycarbonylmethoxy)-calix[4]arene (L2): In dry acetone (10 cm^3), potassium carbonate (0.16 g, 1.2 mmol), 5,11,17,23-tetra-*tert*-butyl-25-(9,10-diphenylanthracene-2-yloxyethoxy)-26,27,28-trihydroxycalix[4]arene (**L1**) (0.20 g, 0.2 mmol) and ethyl bromoacetate (0.2 cm^3, 1.5 mmol) were suspended. The reaction mixture was stirred under reflux in argon atmosphere for 7 days. The resulting mixture was filtrated and the filtrate was evaporated. Dry residue was re-crystallized from ethanol to give 130 mg (54 %) of pure compound **L2**.

Microwave-assisted synthesis of compound **L2** was also performed. 5,11,17,23-tetra-tert-butyl-25-(9,10-diphenylanthracene-2-yloxyethoxy)-26,27,28-trihydroxycalix-[4]arene (**L1**) (0.14 g, 0.1 mmol), potassium carbonate (0.46 g, 3.3 mmol), potassium iodide (0.16 g, 0.9 mmol), 5,11,17,23-tetra-*tert*-butyl-25,26,27,28-tetrahydroxycalix-[4]arene (0.10 g, 0.2 mmol), and ethyl bromoacetate (0.14 g, 0.9 mmol) were suspended in 10 cm^3 of acetonitrile. Reaction mixture was stirred for 2.5 h at 82 °C in microwave reactor. Reaction mixture was evaporated and the dry residue was dissolved in dichloromethane and extracted three times with water to eliminate the salts. Organic layer was evaporated under low pressure and the crude residue was recrystallized from ethanol, yielding 110 mg (78 %) of pure product **L2**.

m. p. 124–126 °C. IR (KBr) $\tilde{\nu}_{max}$ / cm^{-1}: 3057, 2958, 2869, 1757, 1735, 1626, 1477, 1453, 1391, 1367, 1296, 1279, 1231, 1187, 1127, 1068, 1031, 872, 755, 704. ^1H NMR ($CDCl_3$, 600 MHz); δ_H / ppm: 1.07 (s, 9H, C–$(CH_3)_3$); 1.07 (s, 18H, C–$(CH_3)_3$); 1.07 (s, 9H, C–$(CH_3)_3$); 1.20 (t, 4H, J = 7.1 Hz); 1.24 (t, 5H, J = 7.0 Hz); 1.29 (t, 1H, J = 7.1 Hz); 3.12 (d, 2H, J = 12.9 Hz); 3.17 (d, 2H, J = 12.9 Hz); 3.72 (q, 3H, J = 6.9 Hz); 3.97-4.11 (m, 4H); 4.13 (q, 2H, J = 7.1 Hz); 4.21 (q, 1H, J = 7.1 Hz); 4.31 (t, 2H, J = 4.7 Hz); 4.35 (t, 2H, J = 4.3 Hz); 4.62-4.87 (m, 11H); 6.76 (s, 8H, Ar); 6.93 (d, 1H, J = 2.3 Hz); 7.11 (dd, 1H, J = 9.5 Hz, 2.4 Hz); 7.2-7.31 (m, 2H); 7.46 (d, 2H, J = 6.8 Hz); 7.48 (d, 2H, J = 6.9 Hz); 7.52-7.55 (m, 2H); 7.57-7.61 (m, 6H); 7.65 (d, 1H, J = 8.4 Hz).^{13}C NMR ($CDCl_3$, 150 MHz); δ_C / ppm: 13.5; 13.7; 30.9; 30.9; 31.0; 31.4; 33.3; 59.78; 66.5; 70.8; 70.9; 72.0; 103.3; 119.5; 123.5; 124.6; 124.7; 124.9; 125.9; 126.0; 126.5; 126.9; 126.9; 127.9; 128.1; 128.1; 128.1; 129.9; 130.6; 130.8; 130.8; 132.9; 132.9; 132.9; 133.2; 134.4; 136.7; 138.7; 139.0; 144.5; 144.6; 152.5; 152.56; 152.9; 155.7; 169.9; 170.9. HRMS m / z [**L2**+H]$^+$: 1278.6789, calculated for $C_{84}H_{94}O_{11}$: 1278.6790.

Physicochemical Measurements

MATERIALS

The salts used for the investigation of **L1** and **L2** complexation were $LiClO_4$ (Sigma Aldrich, 99.99 %), $NaClO_4$ (Sigma Aldrich 98+ %), Na[B(Ph)$_4$] (Sigma Aldrich, 99.5+ %), $KClO_4$ (Merck, *p.a.*), K[B(Ph)$_4$] (Sigma Aldrich, 97 %), KCl (Merck, 99.5 %), RbCl (Sigma-Aldrich, 99 %), Rb[B(Ph)$_4$] (Sigma Aldrich, 95 %), and RbI (Sigma-Aldrich, 99.9 %). The solvents, acetonitrile (Merck, Uvasol) and methanol (Merck, Uvasol), were used without further purification, whereas dichloromethane (Fluka, Merck) was distilled twice. In potentiometric measurements ionic strength was kept constant at 0.01 mol dm^{-3} by addition of Et_4NClO_4 (Fluka, *p.a.*).

SPECTROPHOTOMETRY AND FLUORIMETRY

UV titrations were performed by means of a Varian Cary 5 double-beam spectrophotometer whereas fluorimetric measurements were carried out using a PekinElmer LS-55 spectrofluorimeter, both equipped with a thermostatting device. UV and fluorescence spectra were recorded at 0.5 nm intervals at 25.0 °C using 1 cm optical path length quartz cells. Spectral changes of solutions of **L1** and **L2** were recorded upon stepwise additions of an alkali metal salt solution directly into the measuring cell. Absorbances were sampled with an integration time of 0.2 s, whereas fluorescence intensities were collected with scanning speed of 600 nm min^{-1}. Titrations for each M^+/**L** system (M^+ stands for alkali metal cation and **L** denotes ligand **L1** or **L2**) were done in triplicate. The obtained data were processed using the SPECFIT[32–34] and HYPERQUAD[35] programs. In the course of spectrophotometric and spectrofluorimetric determinations of stability constants, ion-association was taken into account.[11]

POTENTIOMETRY

For potentiometric measurements, Metrohm 713 pH meter was used. Titrations were carried out in thermostated vessel (ϑ = (25.0 ± 0.1) °C), and the ionic strength of all solutions was kept at 0.01 mol dm^{-3} by addition of Et_4NClO_4. The indicator electrode was a sodium-selective glass electrode (Metrohm, 6.0501.100) with Ag/AgCl reference electrode (Metrohm, 6.0733.100) filled with acetonitrile/dichloromethane solution of Et_4NCl (c = 0.01 mol dm^{-3}). The working and reference half-cells were connected with a salt bridge containing 0.01 mol dm^{-3} Et_4NClO_4. The cell was calibrated by the incremental addition of $NaClO_4$ solution (c = 0.01 mol dm^{-3}) to 30.0 cm^3 solution of Et_4NClO_4 (c = 0.01 mol dm^{-3}) in acetonitrile/dichloromethane mixture (φ = 0.5). A Nernst-like behavior was observed, with the slope of E *vs.* p[Na] plot being about –58 mV.

Stability constant of Na**L2**$^+$ complex in acetonitrile/dichloromethane mixture was determined by potentiometric titration of $NaClO_4$ solution (V = 30.3 cm^3) with solution of **L2** (c = 1.02 × 10^{-2} mol dm^{-3}). Titration was repeated three times, and the obtained potentiometric data were analyzed with the HYPERQUAD program.[35]

CALORIMETRY

Microcalorimetric measurements were performed by an isothermal titration calorimeter Microcal VP-ITC at 25.0 °C. In the calorimetric titrations, the enthalpy changes obtained upon stepwise, automatic addition of alkali metal salt solution (c = 2 × 10^{-3} mol dm^{-3} to 3 × 10^{-3} mol dm^{-3} to) to solution of **L2** (c = 1 × 10^{-4} mol dm^{-3} to 3 × 10^{-4} mol dm^{-3}) were recorded. The anions of alkali metal salts were either tetraphenylborates or perchlorates, *i.e.* large ions with the low charge density and the low tendency for ion-pairing. In this way the extent of the latter process was significantly reduced or even almost completely eliminated. For that reason, the contribution of ion-pair dissociation to the recorded enthalpy changes and its influence on the complexation equilibrium could be neglected in all cases. Blank experiments were performed in order to make corrections for the enthalpy changes corresponding to titrant dilution in pure solvent. The dependence of successive enthalpy change on the titrant volume was processed by non-linear least-square fitting procedure using OriginPro 7.5 program.[36] Titrations for each cation/ligand system were done in triplicate.

Molecular Dynamics Simulations

The molecular dynamics simulations were carried out by means of the GROMACS[37–43] package (version 5.1.4). Intramolecular and nonbonded intermolecular interactions in calixarene ligand and in acetonitrile molecules were modelled by the OPLS-AA (Optimized Parameters for Liquid Simulations-All Atoms) force field.[44] Partial charges assigned to ring carbons bound to CH_2 groups that link the monomers were assumed to be zero. Partial charges of 9,10-diphenylanthracene atoms where calculated for a model compound of 1-ethoxy-9,10-diphenylanthracene with Gaussian 09 software at B3LYP/6–31+G level of theory using a CHelpG scheme.[45] The initial structure of free ligand was the one in which calixarene basket had a conformation of a flattened *cone*. Bond stretching and angle bending parameters for CH_2Cl_2 molecule were taken from Ref. 46. The initial structures of calixarene complexes were built by placing a cation in the center of lower rim cavity between ether and carbonyl oxygen atoms. The M**L2**$^+$ species (M^+ denotes alkali metal cation) were solvated in a cubical box (edge length 65 Å) of acetonitrile/dichloromethane or methanol/dichloromethane mixture with periodic boundary conditions. The compositions of solvents were similar to those used in the experimental studies. The solvent mixture boxes where equilibrated prior to solvation of calixarene ligand and its complexes. Solute concentration in such a box was about 0.01 mol dm^{-3}. During the simulations of the systems ClO_4^- ion was included to neutralize the box. The perchlorate counterion was held fixed at the box periphery whereas the complex was initially positioned at the box center. In all simulations an energy minimization procedure was performed followed by a molecular dynamics simulation in *NpT* conditions, where first 0.5 ns were not used in the data analysis The Verlet algorithm[47] with a time step of 1 fs was employed. The cutoff radius for nonbonded van der Waals and short-range Coulomb interactions was 16 Å. Long-range Coulomb interactions were treated by the Ewald method as implemented in the PME (Particle Mesh Ewald) procedure.[48] The simulation temperature was kept at

298.15 K with Nosé-Hoover[49–50] algorithm using a time constant of 1 ps. The pressure was kept at 1 bar by Martyna-Tuckerman-Tobias-Klein[51] algorithm and a time constant of 1 ps. Figures of calixarene molecular structures were created using VMD software.[52] The simulations of same system where repeated several time in order to accumulate total simulation time adequate for proper data analysis.

Quantum Chemical Calculations

Conformational search for acetonitrile adducts of **L2** complex with Na^+ was performed by calculation of complete potential energy surface (PES) around selected torsional coordinates. PES was spanned by 11 relevant torsional coordinates φ_1–φ_{11} (Figure 1). Torsional coordinates were investigated in the relative range of 0–120° starting from the initial structure. PES scans were obtained by varying the torsional coordinates using the automatic conformational generator implemented in program ***qcc***.[53–57] All single point calculations were conducted at the PM6 semiempirical level of the theory using MOPAC2016.[58–59]

Data from PES scans were arranged in an 11-way array. Parallelized combinatorial optimization algorithm for the arbitrary number of ways (dimensions) implemented in program ***moonee***[60–63] was used to determine all local minima on the investigated PES. All local minima were reoptimized at the B3LYP/3-21G level of the theory whereas the conformers were reoptimized using B3LYP-D3/6-31G(d) level of the theory. To ensure that the obtained conformers indeed corresponded to local minima, harmonic frequency calculations were performed. The standard Gibbs energies were calculated at T = 298.15 K and p = 101325 Pa. All quantum-chemical calculations were performed using the Gaussian 09 program.[45]

RESULTS AND DISCUSSION

Synthesis

Compound **L1**, a monosubstituted calix[4]arene derivative was obtained by reaction of 2-(2-bromoethoxy)-9,10-diphenylanthracene with 5,11,17,23-tetra-*tert*-butyl-25,26,27,28-tetrahydroxycalix[4]arene, as shown in Scheme 2. Calixarene derivative **L2** was prepared by introducing ethoxycarbonylmethoxy groups to the three remaining unsubstituted OH groups of compound **L1** by reaction with ethyl bromoacetate (Scheme 2).

It is well known that the result of alkylation reaction of calixarene is determined with the amount of alkylating agents and type of the base used. This was also the case with the synthesis of diphenylanthracene calix[4]arene derivatives studied. 2.2 equivalents of 2-(2-bromethoxy)-9,10-diphenylanthracene were added to the reaction mixture of 5,11,17,23-tetra-*tert*-butyl-25,26,27,28-tetrahydroxycalix[4]arene resulting in exclusive formation of monosubstituted derivative, compound **L1**. Monosubstituted derivative was further modified by reaction with 2.2 equivalents of ethyl bromoacetate per free OH group giving compound **L2** respectively. Both of the calix[4]arene derivatives were prepared in such reaction conditions (K_2CO_3 as week base, acetone or acetonitrile as solvents) to yield products solely in the *cone* conformation, which was confirmed by NMR spectra (Supporting Information) and is also in agreement with literature data.[64,65] Synthesis of the studied calixarene derivatives was also conducted by microwave assisted heating, using the similar reaction conditions as in the case of conventional synthesis. Microwave-assisted synthesis gave about 20 % higher yields compared to conventional synthesis. Also, notable reduction in reaction times was accomplished (Table 1), which is, considering the fact that reactions of calixarene lower rim modification are generally very time consuming, a significant advantage of the microwave assisted synthesis. Furthermore, it was shown that this method does not demand inert atmosphere and nonaqueous conditions (which are inevitable in conventional synthesis) since yields of reactions of the same duration were approximately the same with and without the use of such conditions.

^{1}H NMR spectrum of compound **L1** (Figure S3, Supporting Information) contained signals corresponding to *tert*-butyl protons split into three singlets with relative intensity ratio 1:2:1, which is a characteristic pattern for monosubstituted calixarene derivatives.[66] Also, the spectrum showed four sets of doublets (δ = 3.37, 3.39, 4.18, and 4.45 ppm) corresponding to protons of methylene bridges confirming that the calixarene derivative had assumed the *cone* conformation. This was expected since three free OH groups can form hydrogen bonds that stabilize this conformation. Furthermore, OH groups signals split into two singlets with intensity ratio 2:1 at high values of chemical shifts (δ = 9.32 and 10.10 ppm), which was yet another confirmation of the existence of intramolecular hydrogen bonds. If this ^{1}H NMR spectrum is compared to that of 2-(2-bromethoxy)-9,10-diphenylanthracene (Figure S1, Supporting Information) the shift of the triplet signal corresponding to O–CH_2–CH_2–O protons to the higher field is notable, also as the result of formation of hydrogen bonds.

^{1}H NMR spectrum of compound **L2** (Figure S5, Supporting Information) is more complex than that of compound **L1** (additional groups present) but pattern in signals corresponding to *tert*-butyl protons and four doublets corresponding to methylene bridges protons appeared, confirming that this derivative is in the *cone* conformation as well.

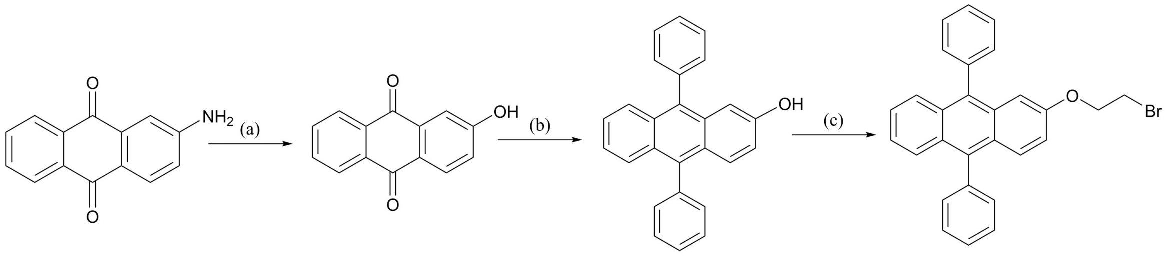

Scheme 1. Synthesis of 2-(2-bromoethoxy)-9,10-diphenylanthracene. Reagents and conditions: a) 1: H_2SO_4, $NaNO_2$, rt, 2: H_2O, Δ; (b) *t*BuLi, bromobenzene,THF(Ar), –60 °C, rt, NH_4Cl(aq), Et_2O, HI, Δ; (c) 1,2-dibromoethane, K_2CO_3, MeCN, Δ.

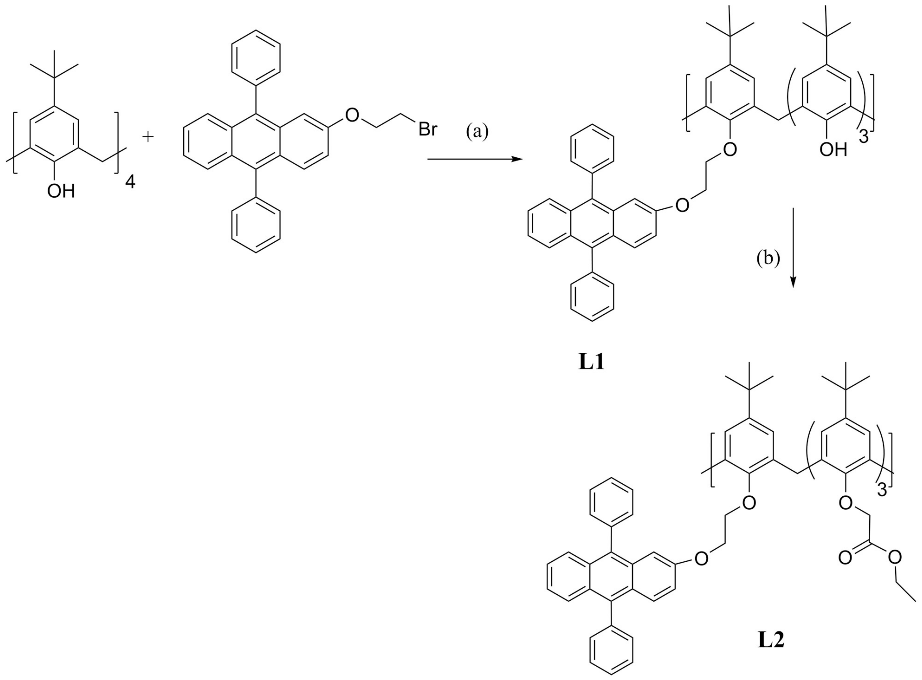

Scheme 2. Synthesis of compounds **L1** and **L2.** Reagents and conditions: a) K_2CO_3, KI, MeCN (Ar) Δ; (b) ethyl bromoacetate, K_2CO_3, KI, acetone (Ar), Δ.

Table 1. Conventional and microwave-assisted synthesis of calix[4]arene derivatives **L1** and **L2**

compound	heating	reaction time / h	reaction yield / %
L1	reflux	120	36
L1	MW	2	56
L2	reflux	168	54
L2	MW	2.5	78

Cation Complexation Studies

Due to the low solubilities of the studied calix[4]arene derivatives in solvents of moderate permittivities, such as acetonitrile or methanol, their complexation abilities towards alkali metal cations were studied in mixed solvent systems, namely MeCN/CH_2Cl_2 and MeOH/CH_2Cl_2 (volume fraction, φ = 0.5).

The binding of cations with **L1** was not observed either spectrophotometrically or fluorimetrically. The addition of alkali metal salts did not cause any changes in the UV or emission spectra of the ligand solutions in both solvent mixtures. This was not surprising considering that **L1** is a diphenylanthracene monosubstituted calixarene which does not possess any other functional groups that could be involved in cation complexation.

The strong fluorescence of **L1** was obviously due to the presence of diphenylanthracene subunit (the **L1** UV and emission spectra closely resembled those of 2-(2-bromo-ethoxy)-9,10-diphenylanthracene; Figure S7, Supporting Information).

SOLVENT: ACETONITRILE/DICHLOROMETHANE (L2)

As example, the results of spectrophotometric titration of **L2** with Na^+ are shown in Figure 2, whereas those

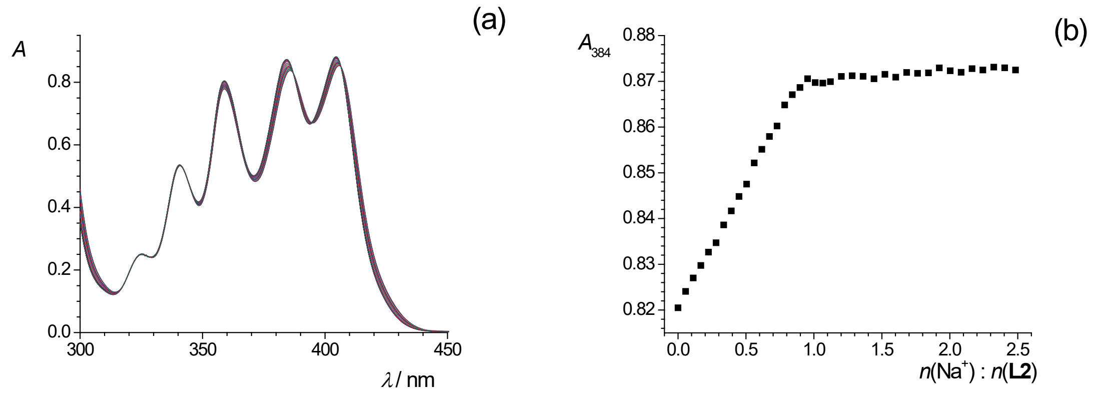

Figure 2. a) Spectrophotometric titration of **L2** ($c = 1.17 \times 10^{-4}$ mol dm^{-3}) with $NaClO_4$ ($c = 1.88 \times 10^{-3}$ mol dm^{-4}) in $MeCN/CH_2Cl_2$ mixture ($\varphi = 0.5$) at 25.0 °C; V_0(**L2**) = 2.0 cm^3; l = 1 cm. Spectra are corrected for dilution. b) absorbance at 384 nm as a function of cation to ligand molar ratio.

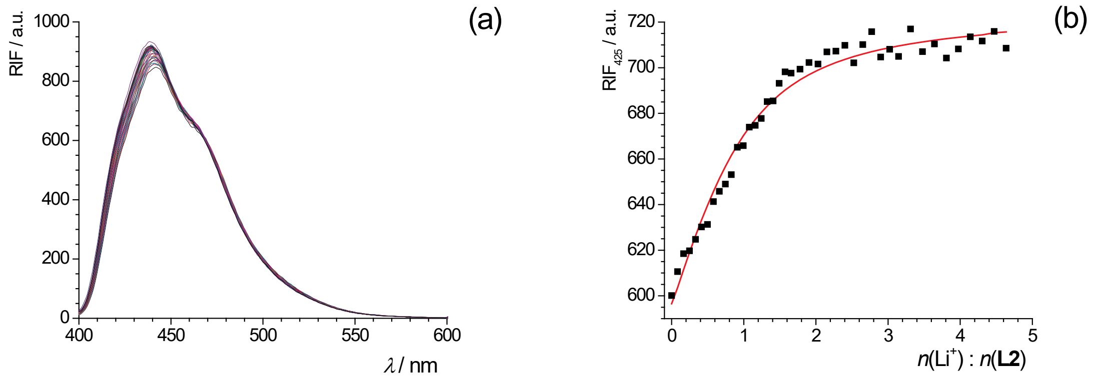

Figure 3. a) Fluorimetric titration of **L2** ($c = 8.63 \times 10^{-7}$ mol dm^{-3}) with $LiClO_4$ ($c = 1.79 \times 10^{-5}$ mol dm^{-3}) in $MeCN/CH_2Cl_2$ mixture ($\varphi = 0.5$) at 25.0 °C; V_0(**L2**) = 2.5 cm^3; l = 1 cm.; λ_{ex} = 384 nm; excitation slit 7 nm, emission slit 3 nm. Spectra are corrected for dilution. b) relative fluorescence intensity at 425 nm as a function of cation to ligand molar ratio; ■ experimental; — calculated.

corresponding to the other alkali metal cations are given in Supporting Information (Figures S8–S10). Spectrophotometric titration curves of **L2** with $LiClO_4$ and $NaClO_4$ exhibited a linear change in absorbance depending of the amount of cation added up to the ratio $n(M^+) / n(\mathbf{L2}) \approx 1$, followed by a break in the titration curve (Figure 2 and Figure S8, Supporting Information). That revealed a formation of 1:1 complexes with high stability constants. As follows from the above considerations, these values were too high for reliable spectrometric determination in $MeCN/CH_2Cl_2$ solvent mixture, and could be only roughly estimated (Table 2). Owing to its larger size, the potassium cation fits less well into the ligand binding site. This allowed for the reliable determination of the corresponding equilibrium constant (and hence the standard reaction Gibbs energy) calculated by a least squares non-linear regression analysis of the spectrophotometric titration data (Table 2, Figure S9, Supporting Information). The addition of rubidium salt into the solution of compound **L2** did not cause any changes in its UV spectrum, indicating that no measurable complexation took place under the conditions used (Figure S10, Supporting Information). This finding was confirmed calorimetrically.

Fluorimetric titrations of ligand **L2** with alkali metal cations were carried out as well. The addition of lithium, sodium or potassium salts to the receptor solution led to an increase in the fluorescence intensity. This effect was ascribed to the inhibition of the photoinduced electron transfer.[9,11,67] However, relatively small changes in fluorescence (as well as in UV absorption) of the ligand was observed upon cation complexation. That can be accounted for by considering the results of quantum chemical calculations which indicated that diphenylanthracene ether oxygen atom was not involved in the cation coordination (see below). Fluorimetric titrations enabled the determination of stability constants for $Li\mathbf{L2}^+$ (Figure 3) and $K\mathbf{L2}^+$ complexes (Figure S12, Supporting Information). It should be noted that the values of $K\mathbf{L2}^+$

stability constant determined by UV and fluorescence spectroscopies are considerably different (Table 2). This inconsistency could be caused by photochemical effects,[68–70] *i.e.* the equilibrium constant determined by emission spectroscopy could correspond to the reaction involving reactants and products in their excited states, or could be a function of both, excited- and ground-state reactions.[71–73]

The stability constant of Na**L2**$^+$ complex in MeCN/CH_2Cl_2 could not be determined reliably by means of flourimetry (Figure S11, Supporting Information). It was hence obtained potentiometrically, using Na^+ selective electrode (Table 2). The corresponding titration curve (Figure 4) was characterized by an inflection point at equivalence, confirming 1:1 stoichiometry of the complex.

The complexation of alkali metal cations with compound **L2** was also investigated microcalorimetrically (Figures S13–S15, Supporting Information). In the cases of the stepwise addition of lithium, sodium or potassium salts negative enthalpy changes were recorded, whereas no heat effects were measured in corresponding experiments involving large alkali metal cations. The standard reaction enthalpies and equilibrium constants (hence the standard reaction Gibbs energies) for the complexation reactions were calculated by a least-squares non-linear regression analysis of the calorimetric titration data. Standard complexation entropies were calculated from the complexation enthalpies and Gibbs energies. As can be seen from the data presented in Table 3, all explored reactions are enthalpically controlled. The standard complexation entropies are negative in all cases except for the reaction with lithium cation. The quite large stability of Li**L2**$^+$ in MeCN/CH_2Cl_2 is a consequence of the favorable enthalpic and quite small, but still positive entropic contribution to the standard complexation Gibbs energy. The latter is likely due to most favorable desolvation of this smallest cation. Namely, because of its considerable charge density, the lithium cation can reorient the solvent dipoles most strongly, even beyond the primary solvation sphere. Its binding to calixarene molecules hence results with the release of larger number solvent molecules into the bulk when compared with the rest of alkali metal cations. On the other hand, the strong interactions of lithium and solvent molecules affects the complexation enthalpy quite unfavorably.

The highest stability of Na**L2**$^+$ in MeCN/CH_2Cl_2 is a consequence of the most favorable enthalpic contribution to the standard complexation Gibbs energy (Table 3). This is quite typical and can be explained by the compatibility of cation and the receptor binding site sizes.[2–4] The much lower stability constant of K**L2**$^+$ compared to the corresponding sodium complex is primarily a consequence of larger reaction enthalpy. The potassium cation is less strongly solvated than sodium one, so its binding should be favored in terms of solvation. Consequently, the difference in the receptor binding affinities towards K^+ and Na^+ can be rationalized by weaker interactions of calixarene donor atoms with K^+ cation. It should be noted that the K**L2**$^+$ stability constant determined calorimetrically is in good agreement with that obtained spectrophotometrically.

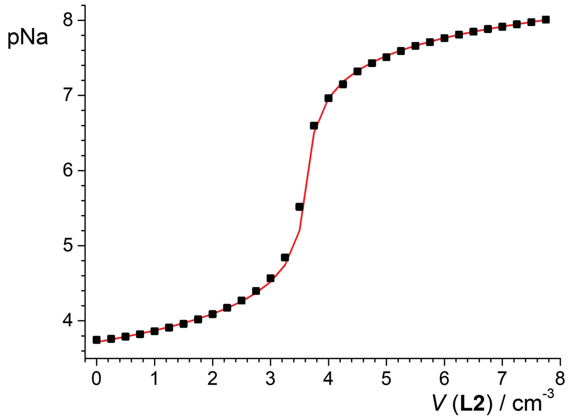

Figure 4. Potentiometric titration of $NaClO_4$ solution ($c = 9.90 \times 10^{-4}$ mol dm^{-3}) with **L2** ($c = 1.02 \times 10^{-2}$ mol dm^{-3}) in MeCN/CH_2Cl_2 solvent mixture ($\varphi = 0.5$) at 25.0 °C; $V_0(NaClO_4) = 30.3$ cm^3; $I_c = 0.01$ mol dm^{-3} (Et_4NClO_4). ■ experimental; — calculated.

Table 2. Stability constants of **L2** complexes with alkali metal cations in MeCN/CH_2Cl_2 ($\varphi = 0.5$) at 25.0 °C determined by different methods

cation	log K(M**L2**$^+$) ± SE		
	UV	fluorimetry	potentiometry
Li^+	>6	6.57 ± 0.01	
Na^+	>6	>7	7.95 ± 0.02
K^+	4.43 ± 0.01	5.15 ± 0.01	

SE = standard error of the mean (N = 3)

There is an additional phenomenon which can considerably contribute to efficient cation hosting in certain solvent. This is the inclusion of the solvent molecule into the hydrophobic calixarene cavity of the ligand and especially of the complex formed[21,22,24,26,27] whereby the particularly favorable interaction between the acetonitrile methyl protons and the electron rich aromatic rings can be realized. In order to explore such a possibility in the studied MeCN/CH_2Cl_2 mixture, the molecular dynamics simulations of the ligand and its alkali metal complexes were performed. In addition, the computational studies provided information regarding the possible structures and dynamics of **L2** and its complexes.

At the beginning of the simulations, the inclusion of solvent molecules in calixarene hydrophobic cavity of both

Table 3. Thermodynamic parameters for complexation of alkali metal cations with **L2** in MeCN/CH_2Cl_2 and MeOH/CH_2Cl_2 (φ = 0.5) obtained by microcalorimetry at 25.0 °C

		MeCN/CH_2Cl_2		
	log $K(\mathrm{M}\mathbf{L2}^+)$ ± SE	$\Delta_r G^\circ$ ± SE / kJ mol^{-1}	$\Delta_r H^\circ$ ± SE / kJ mol^{-1}	$\Delta_r S^\circ$ ± SE / J K^{-1}mol^{-1}
Li^+	6.24 ± 0.01	−35.59 ± 0.04	−34.9 ± 0.3	2 ± 1
Na^+	7.95 ± 0.02[(a)]	−45.37 ± 0.01	−59.56 ± 0.03	−47.4 ± 1
K^+	4.55 ± 0.01	−25.96 ± 0.07	−44.3 ± 0.4	−61 ± 2
		MeOH/CH_2Cl_2		
Na^+	5.18 ± 0.01	−29.56 ± 0 07	−39.1 ± 0.1	−39.2 ± 0.7

(a) determined potentiometrically, SE = standard error of the mean (*N* = 3)

L2 and M**L2**$^+$ species (M stands for alkali metal cation) was observed. In the case of **L2** the calixarene cavity was occupied with MeCN molecule (Figure 21a, Supporting Information) during 90 % of the simulation time, whereas the inclusion of CH_2Cl_2 was hardly noticed (the **L2**CH_2Cl_2 adduct, Figure S21c, Supporting Information, was observed during 2.54 % of the simulation time). The acetonitrile molecule was oriented with the nitrile group pointed towards the bulk. The free **L2** adopted flattened *cone* conformation, which was reflected in the markedly different distances of the opposing aryl carbon atoms that are directly bound to *tert*-butyl groups (Table S1, Supporting Information). After the inclusion of solvent molecule, the shape of the *cone* remained somewhat flattened, although it resembled the regular square *cone* conformation for both acetonitrile and dichloromethane adducts (Table S1, Supporting Information). The interaction energies between **L2** and MeCN or CH_2Cl_2 molecules included in the hydrophobic *basket* of free **L2** were similar being around −50 kJ mol^{-1}. The overall solvation with CH_2Cl_2 molecules was energetically more favorable for all forms of **L2** (Table S2, Supporting Information).

During the MD simulations of alkali metal cation complexes of ligand **L2** in acetonitrile/dichloromethane mixture the release of cation from the complex was observed, which was most pronounced for the potassium cation (dissociation took place on average after 3.5 ns), followed by lithium (13.5 ns) cation. In the case of Na**L2**$^+$ complex the cation release was observed only after 53 ns of simulation time. The average dissociation time can be directly correlated with the experimentally determined stability constants measurements (Table 2), namely more stable complexes dissociated after longer period of time. All of the complexes were stable in the course of MD simulations in vacuo during 100 ns. To find out whether the force fields parameters for diphenylanthracene moiety influenced cation binding properties of **L2** observed by MD simulations, two model calixarene ligands were simulated, namely tetra-ester derivative and the one in which the diphenylanthracene in **L2** was replaced by a methyl group. In all these simulations the alkali metal cations were again released from the complex after some time. The observed phenomenon could serve as a clear indication that the OPLS–AA force field parameters used for model bonded and non–bonded interactions were not apt for the appropriate thermodynamic description of M**L2**$^+$ species. That could be also concluded for alkali metal cation complexes of any ligand comprising lower rim substituents with ester groups in the solvent mixture studied. Nevertheless, the M**L2**$^+$ complexes could be considered as thermodynamically metastable species during the initial period of simulation, thus at least some information on their structures and interaction energies between system components can be deduced from the obtained trajectories.

During the simulations of alkali metal cation complexes of **L2** the inclusion of solvent molecules was highly pronounced, whereby the calixarene hydrophobic cavity of M**L2**$^+$ species was occupied by the solvent molecule for the most of the simulation time during which the complex existed (Tables S3–S5, Figures 6, S21–S23, Supporting Information). As was the case with the uncomplexed **L2**, acetonitrile adducts of its complexes were much more stable than those comprising dichloromethane molecules, and were present for the most of the simulation time (Tables S3–S5, Supporting Information). The conformation of the calixarene *basket* in M**L2**MeCN$^+$ species was very close to the square *cone* (Tables S3–S5, Supporting Information), being most regular for Na**L2**MeCN$^+$ adduct. The cations were coordinated by phenolic and carbonyl oxygen atoms as well as by diphenylanthracene ether oxygen atom (Tables S3–S5, Supporting Information). Sodium and potassium cations were coordinated with ≈2.8 carbonyl oxygen atoms on average, whereas for Li^+ the corresponding coordination number amounted to only ≈1.8.

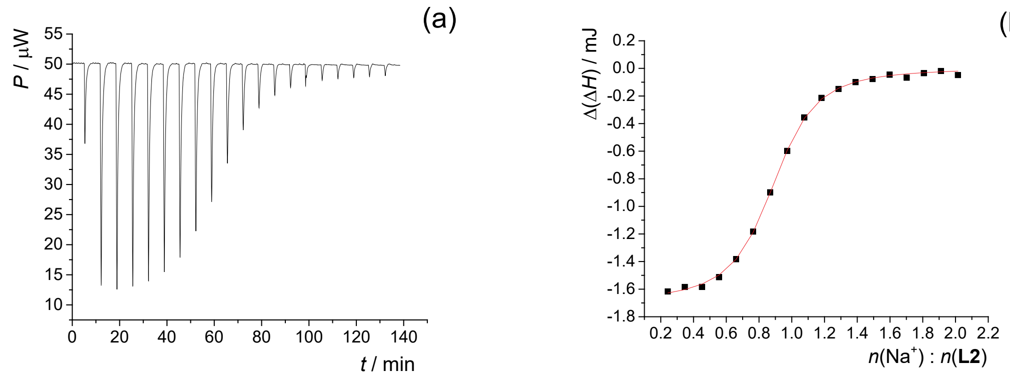

Figure 5. a) Microcalorimetric titration of **L2** (c = 2.95 × 10^{-4} mol dm^{-3}, V = 1.42 ml) with $Na[B(Ph)_4]$ (c = 2.92 × 10^{-3} mol dm^{-3}) in $MeOH/CH_2Cl_2$ solvent mixture (φ = 0.5) at 25 °C; b) Dependence of successive enthalpy change on cation to ligand molar ratio. ■ experimental; — calculated.

The interaction of calixarene ligand with alkali metal cation is weaker as the cation size increases (Tables S3–S6, Supporting Information).

SOLVENT: METHANOL/DICHLOROMETHANE (L2)

The complexation of Li^+ with **L2** in $MeOH/CH_2Cl_2$ solvent mixture could not be observed either spectrometrically or flourimetrically. This is in accordance with previously reported results involving calix[4]arene derivatives in this solvent as well as in pure methanol[11,19,21] and can be attributed to particularly strong cation solvation with this alcohol.[74] The addition of Na^+ or K^+ salt solutions to the solution of compound **L2** caused a small increase in the absorbance with the appearance of several isosbestic points, pointing to the equilibrium between two spectrally active species, namely the free ligand and the complexed ligand (Figures S16 and S17, Supporting Information). The stability constants obtained by processing spectrometric and fluorimetric data are listed in Table 4. By comparing these data with those provided in Table 3, one can observe notable decrease in the affinity of the receptor towards both cations. Again the values corresponding to $K\mathbf{L2}^+$ complex determined by the two methods are quite different, which can be explained in the same way as previously in the case of $MeCN/CH_2Cl_2$ mixture as a solvent. In order to explore complexation thermodynamics in more detail, the binding of sodium cation by **L2** was also investigated microcalorimetrically (Figure 5). Unfortunately, due to the rather low stability of $K\mathbf{L2}^+$ complex and poor solubility of potassium salt used in calorimetric experiments, the reliable calorimetric determination of the corresponding thermodynamic quantities could not be realized in $MeOH/CH_2Cl_2$ solvent mixture. The calorimetric data for the complexation of sodium cation (Tables 3 and 4) reveal much less enthalpically favorable cation binding in $MeOH/CH_2Cl_2$ in comparison to $MeCN/CH_2Cl_2$. On the other hand, the complexation is entropically slightly favored in the former solvent mixture.

Table 4. Stability constants of **L2** complexes with alkali metal cations in $MeOH/CH_2Cl_2$ (φ = 0.5) at 25.0 °C obtained by UV and fluorimetric titrations

cation	log $K(M\mathbf{L2}^+)$ ± SE	
	UV	fluorimetry
Na^+	5.49 ± 0.01	5.50 ± 0.05
K^+	2.95 ± 0.01	3.37 ± 0.01

SE = standard error of the mean (N = 3)

The above findings could be explained by taking into account the more energetically demanding desolvation of Na^+ in $MeOH/CH_2Cl_2$, as well as stronger affinity of the complexed ligand hydrophobic basket for acetonitrile molecule compared to the methanol one.

As in the case of $MeCN/CH_2Cl_2$ as a solvent, titrations of compound **L2** with Rb^+ in $MeOH/CH_2Cl_2$ mixture led to no changes in the UV spectrum under the experimental conditions used (Figure S18, Supporting Information). The complexation of this cation could also not be observed calorimetrically.

The structure of calixarene **L2** and its cation complexes in methanol/dichloromethane mixture was also explored by means of molecular dynamics simulations. During these simulations a release of cation was observed as in the case in acetonitrile/dichloromethane solvent, and again the complex dissociation time followed the trend of experimentally determined stability constants. The dissociation also occurred in the cases of alkali metal cation complexes of two model compounds that were studied in $MeCN/CH_2Cl_2$ solvent.

For **L2** and its cation complexes the inclusion of methanol and dichloromethane molecules in the calixarene

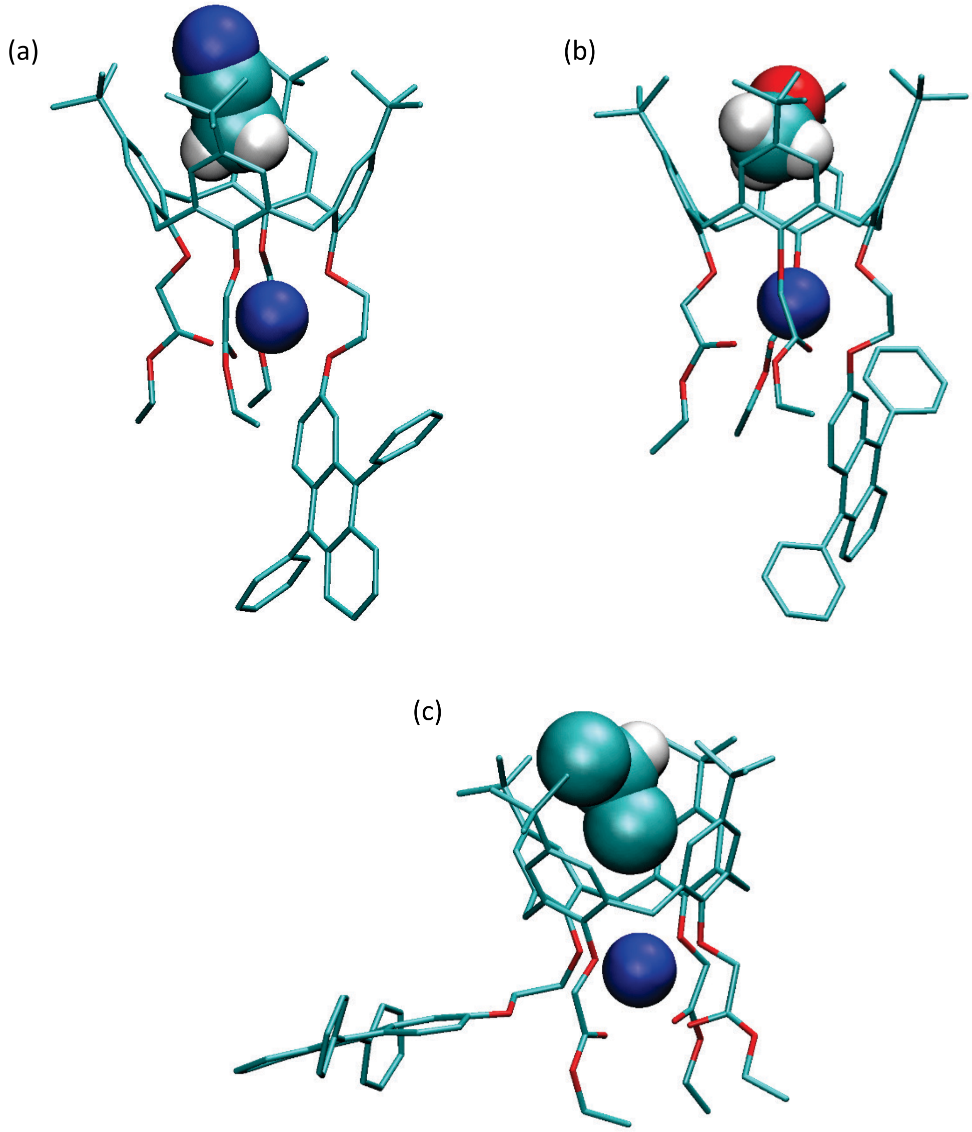

Figure 6. Molecular structures of a) Na**L2**MeCN$^+$, b) Na**L2**MeOH$^+$ and c) Na**L2**$CH_2Cl_2^+$ adducts obtained by MD simulations of Na**L2**$^+$ in acetonitrile/dichloromethane and methanol/dichloromethane mixtures at 25 °C. Hydrogen atoms bound to carbon atoms of **L2** have been omitted for clarity.

basket was observed (Figures 6, S21–S23, Supporting Information), and upon that the macrocycle hydrophobic *cone* became more regular than that of the free ligand (Tables S7–S9, Supporting Information). In the **L2**MeOH and all of the M**L2**MeOH$^+$ adducts the methyl group of methanol molecule was oriented towards the calixarene lower rim. The binding mode of the solvent molecule was similar to that previously found by the MD simulations of different calixarene–methanol adducts.[22,24] The calixarene cavity was occupied with MeOH approximately 2–5 times longer period of time than with CH_2Cl_2 (Tables S6–S7, Supporting Information). The solvent–ligand interaction energy in metal ion complexes and the corresponding adducts was about twice lower for dichloromethane than methanol (Tables S6–S7, Supporting Information). The coordination spheres of cations consisted of phenolic oxygen atoms and variable number of carbonyl and diphenylanthracene ether oxygen atoms. As in the case of the MD simulations of **L2** cation complexes in acetonitrile/dichloromethane mixture, in methanol/dichloromethane the interaction of calixarene ligand with alkali metal cations was found to be less favorable for larger cation in all examined complex species (Tables S6–S7, Supporting Information).

Quantum Chemical Calculation

Initial set of geometries for the conformational analysis of Na**L2**MeCN$^+$ species was obtained by the analysis of PES calculated at the semiempirical level of the theory (PM6). PES was spanned in the space of 11 torsional coordinates (Figure 7) and then parallelized optimization procedure for finding local minima utilizing a brute-force search in *n*-way space was applied and 17 local minima were found. Each local minimum found at the semiempirical level was subsequently optimized using density functional theory. The clustering procedure for the optimized geometries of local minima provided nine distinct conformers, which were then optimized at the B3LYP-D3/6-31G(d) level of theory. For these conformers harmonic frequency calculations were carried out and standard Gibbs energies were calculated. Two conformers of minimal energy are presented in Figure 7.

In both conformers the position of the Na$^+$ cation inside the calixarene is determined by the position of acetonitrile molecule in the hydrophobic calixarene *cone*. The acetonitrile molecule symmetrizes the chemical environment of sodium cation ensuring the proper configuration of the oxygen donor atoms. If acetonitrile molecule moves upwards, the local symmetry around the cation is broken and the standard Gibbs energy of formation is much higher. In each case the position of anthracene subunit is directed outside of the lower rim resulting with a minimum of steric hindrances.

In the lowest energy conformer, distances between phenolic oxygen atoms and Na$^+$ cation were in the range from 2.22 to 2.29 Å. Similar values were obtained for carbonyl oxygen atoms, whereas in the case of ester oxygen atoms these values were much higher (≈2.7 Å). Since in the calculated conformational space there was no low-energy conformer where the diphenylanthracene ether oxygen atoms could be considered as one of the coordinating oxygen atoms for Na$^+$, it is highly unlikely that this atom participates in cation complexation. Structures of additional conformers are given in the Supporting Information (Figure S24).

CONCLUSION

The complexation of alkali metal cations by two novel fluorescent lower-rim calix[4]arenes containing diphenylanthracene moiety was studied in acetonitrile/dichloromethane and methanol/dichlormethane mixtures (φ = 0.5) by means of microcalorimetric, spectrophotometric and flourimetric titrations. Classical molecular dynamics and quantum chemical calculations were carried out as well. The binding of alkali metal cations with monosubstituted calixarene derivative (**L1**) was not observed in either of the

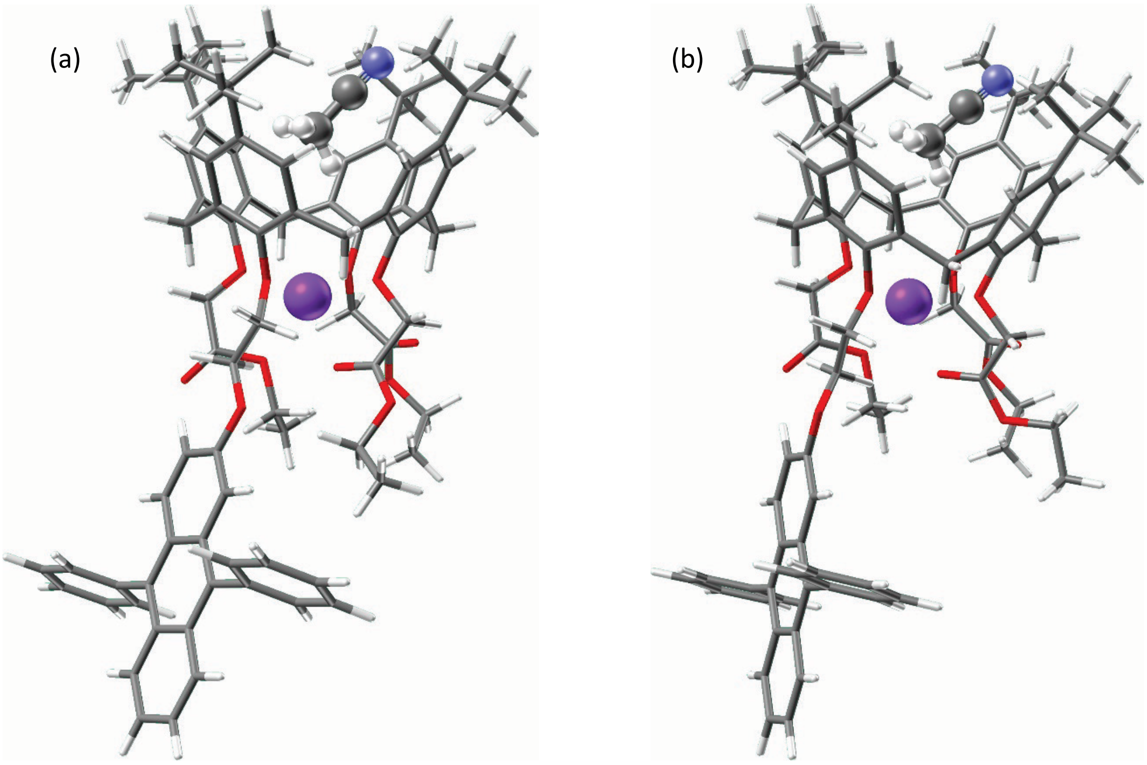

Figure 7. Two lowest energy conformers of Na**L2**MeCN$^+$ species; $\Delta_fG°$ = 25.80 kJ mol^{-1} (relative to the lowest energy conformer).

solvent mixtures. In contrast, the macrocycle **L2**, additionally possessing three ester subunits, exhibited rather high affinity towards lithium, sodium and potassium cations in $MeCN/CH_2Cl_2$, whereas its cation binding ability was found to be considerably lower in $MeOH/CH_2Cl_2$. All reactions involving receptor **L2** were enthalpically controlled. The sodium complex of **L2** was the most stable in both studied solvents. That could be attributed to the energetically most favorable host-guest interactions which was due to compatibility of the cation and the receptor binding site sizes. The inclusion of solvent molecules in the hydrophobic *basket* of **L2** and its cation complexes was observed by MD simulations. The affinity of complexes for methanol and acetonitrile inclusion was higher as compared to that of the free ligand, and was more pronounced in the case of acetonitrile. These findings could serve to (at least partly) explain notably more favorable cation complexation in $MeCN/CH_2Cl_2$ than $MeOH/CH_2Cl_2$ in solvent mixture.[11,24]

The computational investigations provided information regarding the possible structures of compound **L2** and its complexes. The results of quantum chemical calculations indicated that diphenylanthracene ether oxygen atom was not involved in the coordination of sodium cation in the Na**L2**$MeCN^+$ complex species. This fact is most likely the reason for the rather small changes in UV and fluorescence spectra observed upon the reaction of the ligand and Na^+ cation. Similar can be concluded for the other alkali metal cations.

Acknowledgment. This work has been fully supported by Croatian Science Foundation under the project IP-2014-09-7309 (SupraCAR). Computational resources provided by the Croatian National Grid Infrastructure (www.cro-ngi.hr) at Zagreb University Computing Centre (Srce) were used for this publication.

Supplementary Information. Supporting information to the paper is attached to the electronic version of the article at: https://doi.org/10.5562/cca3308.

REFERENCES

[1] Gutsche, C. D. *Calixarenes: An Introduction*; 2nd ed., The Royal Society of Chemistry: Cambridge, UK, 2008.

[2] B. S. Creaven, D. F. Donlon, J. McGinley, *Coord. Chem. Rev.* **2009**, *253*, 893−962.

[3] W. Sliwa, T. Girek, *J. Incl. Phenom. Macrocycl. Chem.* **2010**, *66*, 15–41.

[4] A. F. Danil de Namor, R. M. Cleverley, M. L. Zapata-Ormachea, *Chem. Rev.* **1998**, *98*, 2495−2525.

[5] Z. Asfari, V. Böhmer, J. Harrowfield, J. Vicens, *Calixarenes 2001;* Kluwer Academic Publishers: Dordrecht, 2001.

[6] I. Sviben, N. Galić, V. Tomišić, L. Frkanec, *New J. Chem.* **2015**, *39*, 6099–6107.

[7] B. Mokhtari, K. Pourabdollah, N. Dalali, *J. Incl. Phenom. Macrocycl. Chem.* **2011**, *69*, 1–55.

[8] D. M. Homden, C. Redshaw, *Chem. Rev.* **2008**, *108*, 5086–5130.

[9] J. S. Kim, D. T. Quang, *Chem. Rev*. **2007**, *107*, 3780–3799.

[10] B. Mokhtari, K.Pourabdollah, N. Dalali, *J. Incl. Phenom. Macrocycl. Chem.* **2011**, *69*, 1–55.

[11] M. Tranfić Bakić, D. Jadreško, T. Hrenar, G. Horvat, J. Požar, N. Galić, V. Sokol, R. Tomaš, S. Alihodžić, M. Žinić, L. Frkanec, V. Tomišić, *RSC Adv.* **2015**, *5,* 23900–23914.

[12] F. Nasuhi Pur, *Mol. Divers*. **2016**, *20*, 781–787.

[13] C. Mareque Rivas, H. Schwalbe, S. J. Lippard, *Proc. Natl. Acad. Sci. USA,* **2001**, *98*, 9478.

[14] S. E. Matthewsa, P. D. Beerb in *Calixarenes in the Nanoworld* (Eds.: J. Vicens and J. Harrowfield), Springer, 2007. pp. 109–133.

[15] Z. Xu, S. Peng, Y. Y. Wang, J.-K.Zhang , A. I. Lazar D.-S. Guo, *Adv.Mater*. **2016**, *28*, 7666–7671.

[16] A. R. Kongor, V. A Mehta, K. M. Modi, M. K. Panchal, S. A. Dey, U. S. Panchal, V. K. Jain, *Top. Curr. Chem.* **2016**, *374*:28.

[17] A. F. Danil de Namor, in: Asfari, Z. Böhmer, V. Harrowfield, J. Vicens, J. (Eds.) *Calixarenes 2001;* Kluwer Academic Publishers: Dordrecht, 2001, pp. 346–364.

[18] A. F. Danil de Namor, T. T. Matsufuji-Yasuda, K. Zegarra-Fernandez, O. A. Webb, A. E. Gamouz, *Croat. Chem. Acta.* **2013**, *86*, 1–19.

[19] J. Požar, T. Preočanin, L. Frkanec, V. Tomišić, *J. Solution Chem*. **2010**, *39*, 835–848.

[20] G. Horvat, V. Stilinović, T. Hrenar, B. Kaitner, L. Frkanec, V. Tomišić, *Inorg. Chem.* **2012**, *51*, 6264–6278.

[21] J. Požar, I. Nikšić-Franjić, M. Cvetnić, K. Leko, N. Cindro, K. Pičuljan, I. Borilović, L. Frkanec, V. Tomišić, *J. Phys. Chem. B*, **2017**, *121* (36), 8539–8550.

[22] G. Horvat, L. Frkanec, N. Cindro,V. Tomišić, *Phys. Chem. Chem. Phys*., **2017**, *19*, 24316–24329.

[23] K. Leko, N. Bregović, M. Cvetnić, N. Cindro, M. Tranfić Bakić, J. Požar, V. Tomišić, *Croat. Chem. Acta.* **2017**, *90*, (2), 307–314.

[24] G. Horvat, V. Stilinović, B. Kaitner, L. Frkanec, V. Tomišić, *Inorg. Chem.* **2013**, *52*, 12702–12.

[25] N. Cindro, J. Požar, D. Barišić, N. Bregović, K. Pičuljan, R. Tomaš, L. Frkanec, V. Tomišić, *Org. Biomol. Chem.*, **2018**, *16*, 904–912.

[26] A. F. D. de Namor, N. A. de Sueros, M. A. McKervey, G. Barrett, F. A. Neu, M. J. Schwing-Weill, *J. Chem. Soc. Chem. Commun.*, **1991**, 1546–1548.

[27] A. S. de Araujo, O. E. Piro, E. E. Castellano, A. F. Danil de Namor, *J. Phys. Chem. A*, **2008**, *112*, 11885–11894.

[28] N. Galić, N. Burić, R. Tomaš, L. Frkanec, V. Tomišić, *Supramol. Chem.*, **2011**, *23*, 389–397.

[29] M. Kumar, J. N. Babu, V. Bhalla, R. Kumar, *Sensors Actuators B Chem.*, **2010**, *144*, 183–191.

[30] J. Vicens, J. Harrowfield and L. Baklouti, Eds., *Calixarenes in the Nanoworld*, Springer, 2007.

[31] A. I. Vogel's, *Textbook of Practical Organic Chemistry*, 4th Edition, Longman, 1978.

[32] H. Gampp, M. Maeder, C. J. Meyer, A. D. Zuberbuhler, *Talanta*, **1985**, *32*, 95–101.

[33] H. Gampp, M. Maeder, C. J. Meyer, A. D. Zuberbuhler, *Talanta*, **1985**, *32*, 257–264.

[34] M. Maeder, A. D. Zuberbuhler, *Anal. Chem.*, **1990**, *62*, 2220–2224.

[35] P. Gans, A. Sabatini, A.Vacca, *Talanta,* **1996**, *43*, 1739–1753.

[36] Origin 7.5. OriginLab Corp., Northampton, MA, http://www.originlab.com.

[37] H. J. C. Berendsen, D. van der Spoel, R. van Drunen, *Comput. Phys. Commun.*, **1995**, *91*, 43–56.

[38] E. Lindahl, B. Hess, D. van der Spoel, *J. Mol. Model.* **2001**, *7,* 306–317.

[39] D. Van Der Spoel, E. Lindahl, B. Hess, G. Groenhof, A. E. Mark, H. J. C. Berendsen, *J. Comput. Chem.*, **2005**, *26*, 1701–1718.

[40] B. Hess, C. Kutzner, D. van der Spoel, E. Lindahl, *J. Chem. Theory Comput.*, **2008**, *4*, 435–447.

[41] S. Pronk, S. Páll, R. Schulz, P. Larsson, P. Bjelkmar, R. Apostolov, M. R. Shirts, J. C. Smith, P. M. Kasson, D. van der Spoel, B. Hess, E. Lindahl, *Bioinformatics*, **2013**, *29*, 845–854.

[42] S. Páll, M. J. Abraham, C. Kutzner, B. Hess, E. Lindahl, *Lect. Notes Comput. Sci.* **2015**, 3–27.

[43] M. J. Abraham, T. Murtola, R. Schulz, S. Páll, J.C. Smith, B. Hess, E. Lindahl, *Software X,* **2015**, *1–2*, 19–25.

[44] W. L. Jorgensen, D. S. Maxwell, J. Tirado-Rives, *J. Am. Chem. Soc.*, **1996**, *118*, 11225–11236.

[45] Gaussian 09, Revision D.01, M. J. Frisch, G. W. Trucks, H. B. Schlegel, G. E. Scuseria, M. A. Robb, J. R. Cheeseman, G. Scalmani, V. Barone, B. Mennucci, G. A. Petersson, H. Nakatsuji, M. Caricato, X. Li, H. P. Hratchian, A. F. Izmaylov, J. Bloino, G. Zheng, J. L. Sonnenberg, M. Hada, M. Ehara, K. Toyota, R. Fukuda, J. Hasegawa, M. Ishida, T. Nakajima, Y. Honda, O. Kitao, H. Nakai, T. Vreven, J. Montgomery, J. A., J. E. Peralta, F. Ogliaro, M. Bearpark, J. J. Heyd, E. Brothers, K. N. Kudin, V. N. Staroverov, R. Kobayashi, J. Normand, K. Raghavachari, A. Rendell, J. C. Burant, S. S. Iyengar, J. Tomasi, M. Cossi, N. Rega, M. J. Millam, M. Klene, J. E. Knox, J. B. Cross, V. Bakken, C. Adamo, J. Jaramillo, R. Gomperts, R. E. Stratmann, O. Yazyev, A. J. Austin, R. Cammi, C. Pomelli, J. W. Ochterski, R. L. Martin, K. Morokuma, V. G. Zakrzewski, G. A. Voth, P. Salvador, J. J. Dannenberg, S. Dapprich, A. D. Daniels, Ö. Farkas, J. B. Foresman, J. V. Ortiz, J. Cioslowski, Gaussian Inc., Wallingford CT, 2013.

[46] L. X. Dang, *J. Phys. Chem. B*, **2001**, *105*, 804–809.

[47] W. C. Swope, H. C. Andersen, P. H. Berens, K. R. Wilson, *J. Chem. Phys.*, **1982**, *76*, 637–649.

[48] T. Darden, D. York, L. Pedersen, *J. Chem. Phys.*, **1993**, *98*, 10089–10092.

[49] S. Nosé, *Mol. Phys.*, **1984**, *52*, 255–268.

[50] W. Hoover, *Phys. Rev. A*, **1985**, *31*, 1695–1697.

[51] G. J. Martyna, M. E. Tuckerman, D. J. Tobias, M. L. Klein, *Mol. Phys.*, **1996**, *87*, 1117–1157.

[52] W. Humphrey, A. Dalke, K. Schulten, VMD: Visual molecular dynamics, *J. Mol. Graph.*, **1996**, *14*, 33–38.

[53] T. Hrenar, ***qcc***, *Quantum Chemistry Code*, rev. 0.682, 2018.

[54] T. Hrenar, I. Primožič, D. Fijan, M. Majerić Elenkov, *Phys. Chem. Chem. Phys.*, **2017**, *19* 31706–31713.

[55] I. Primožič, T. Hrenar, K. Baumann, L. Krišto, I. Križić, S. Tomić, *Croat. Chem. Acta,* **2014**, *87*, 155–162.

[56] D. Šišak Jung, T. Hrenar, O. Jović, P. Kalinovčić, I. Primožič, *Powder Diffr.*, **2015**, *30*, S36.

[57] V. Lazić, M. Jurković, T. Jednačak, T. Hrenar, J. Parlov Vuković, P. Novak, *J. Mol. Struct.* **2015**, *1079*, 243–249.

[58] J. J. P. Stewart *J. Mol. Model.* **13** (2007) 1173–1213.

[59] MOPAC2016, J. J. P. Stewart, Stewart Computational Chemistry, Colorado Springs, CO, USA, 2016, http://OpenMOPAC.net

[60] T. Hrenar, ***moonee***, *Code for Manipulation and Analysis of Multi- and Univariate Data*, rev. 0.6826, 2018.

[61] O. Jović, T. Smolić, I. Primožič, T. Hrenar, *Anal. Chem.*, **2016**, *88*, 4516.

[62] J. Parlov Vuković, T. Hrenar, P. Novak, M. Friedrich, J. Plavec, *Energy & Fuels*, **2017**, *31*, 8095–8101.

[63] P. Novak, A. Kišić, T. Hrenar, T. Jednačak, S. Miljanić, G. Verbanec, *J. Pharm. Biomed. Anal.*, **2011**, *54*, 660–666.

[64] M. A. McKervey, E. M. Seward, G. Ferguson, B. Ruhl, S. J. Harrisc, *J. Chem. Soc. Chem. Commun.,* **1985**, 388–390.

[65] F. Arnaud-Neu, S. Fanni, L. Guerra, W. McGregor, K. Ziat, M.-J. Schwing-Weill, G. Barrett, M. A. McKervey, D. Marrs, E. M. Seward, *J. Chem. Soc. Perkin Trans.*, **1995**, *2* ,113–118.

[66] O. A. Omran, *Molecules,* **2009**, *14*, 1755–1761.

[67] B. Valeur, *Molecular Fluorescence: Principles and Applications*, WILEY-VCH, Weinheim, 2001.

[68] V. Blažek, K. Molčanov, K. Mlinarić-Majerski, B. Kojić-Prodić, N. Basarić, *Tetrahedron*, **2013**, *69*, 517–526.

[69] N. Sadlej-Sosnowska, L. Kozerski, E. Bednarek, J. Sitkowski, *J. Incl. Phen. Macrocyc. Chem.,* **2000**, *37*, 383–394.

[70] M. El Baraka, R. García, E. Quinoñes, *J. Photochem. Photobiol. A: Chem.* **1994**, *79*, 181–187.

[71] B. D. Wagner, *Phys. Chem. Chem. Phys.* **2012**, *14,* 8825–8835.

[72] J. F. Ireland, P. A. H. Wyatt, *Adv. Phys. Org. Chem.* **1976**, *12,* 121–221.

[73] N. Bregović, N. Cindro, L. Frkanec, V. Tomišić, *Supramol. Chem*., **2016**, *28,* 608–615.

[74] Y. Marcus, *Ion Properties*, M. Dekker: New York, 1997.